ELSEVIER

Nuclear Instruments and Methods in Physics Research A 490 (2002) 299–307

NUCLEAR INSTRUMENTS & METHODS IN PHYSICS RESEARCH Section A

www.elsevier.com/locate/nima

Pulse shape analysis of liquid scintillators for neutron studies

S. Marrone[a], D. Cano-Ott[b], N. Colonna[a,*], C. Domingo[c], F. Gramegna[d], E.M. Gonzalez[b], F. Gunsing[e], M. Heil[f], F. Käppeler[f], P.F. Mastinu[d], P.M. Milazzo[g], T. Papaevangelou[h], P. Pavlopoulos[i], R. Plag[f], R. Reifarth[f], G. Tagliente[a], J.L. Tain[c], K. Wisshak[f]

[a] *Dipartimento di Fisica, Istituto Nazionale di Fisica Nucleare (INFN), Sezione di Bari, via Amendola 173, I-70126 Bari, Italy*
[b] *CIEMAT, Madrid, Spain*
[c] *Istituto de Fisica Corpuscolar, Universidad de Valencia, Spain*
[d] *Laboratori Nazionali Legnaro, Legnaro, Italy*
[e] *DSM/DAPNIA, CEA, Saclay, Gif-sur-Yvette, France*
[f] *Forschungszentrum Karlsruhe, Institut für Kernphysik, Karlsruhe, Germany*
[g] *Istituto Nazionale di Fisica Nucleare, Sezione di Trieste, Italy*
[h] *Aristotele University, Department of Physics, Thessaloniki, Greece*
[i] *University of Basel, Switzerland*

The n_TOF Collaboration

Received 3 May 2001; received in revised form 6 May 2002; accepted 6 May 2002

Abstract

The acquisition of signals from liquid scintillators with Flash ADC of high sampling rate (1 GS/s) has been investigated. The possibility to record the signal waveform is of great advantage in studies with γ's and neutrons in a high count-rate environment, as it allows to easily identify and separate pile-up events. The shapes of pulses produced by γ-rays and neutrons have been studied for two different liquid scintillators, NE213 and C_6D_6. A 1-parameter fitting procedure is proposed, which allows to extract information on the particle type and energy. The performance of this method in terms of energy resolution and n/γ discrimination is analyzed, together with the capability to identify and resolve pile-up events. © 2002 Elsevier Science B.V. All rights reserved.

PACS: 29.30.Hs; 29.40.Mc; 29.85.+c; 28.20.−v

Keywords: Liquid scintillators; Pulse shape discrimination; Flash ADC; n_TOF

1. Introduction

Liquid scintillator detectors are widely employed in studies with fast neutrons and γ-rays [1–4]. Several properties make such detectors very appealing: the relatively high light-output, a reasonably good efficiency for fast neutrons and the fast decay time of the light output. The last feature is particularly useful in those studies where timing information is required as well as in measurements characterized by high count rates. Furthermore, an additional slow component

*Corresponding author. Tel.: +39-80-544-2351; fax: +39-80-544-2470.

E-mail address: nicola.colonna@ba.infn.it (N. Colonna).

0168-9002/02/$ - see front matter © 2002 Elsevier Science B.V. All rights reserved.
PII: S0168-9002(02)01063-X

which depends on the energy loss density, makes common liquid scintillators suited for neutron–gamma discrimination. Several methods can be used for this purpose. In one of them, information on the particle type is obtained from the zero-crossing time of the suitably shaped signal [5,6]. Alternatively, a double charge integration can be used, with the two integration gates suitably chosen so as to extract the relative contribution of the slow component versus the total light output [7–9]. The performances of the two methods have been extensively analyzed and compared [10,11], even in the presence of pile-up [12], while a new pattern recognition method has also recently been proposed [13].

Although the signals of liquid scintillators are relatively fast, there often exist situations in which the detectors operate in a high count-rate environment, so that pile-up between successive events may occur. In this case, several methods and electronic circuits have been proposed which allow to identify and reject pile-up events, thus restoring the original energy resolution and n/γ discrimination capability [12]. These techniques, however, cannot be applied when pile-up signals constitute a large fraction of the detected events. Furthermore, in high-precision cross-section measurements it is desirable to record and analyze all events, including those that give rise to pile up. This is particularly important for measurements at the new neutron time-of-flight facility n_TOF at CERN [14]. C_6D_6-based liquid scintillators, characterized by a small sensitivity to low-energy neutrons, will be used to measure (n,γ) cross-sections relevant for Astrophysics and for applications to Accelerator Driven Systems for energy production and nuclear waste incineration [15]. The high instantaneous intensity of the neutron beam at the n_TOF facility is predicted to result in a large probability of pile-up events, and an appropriate strategy has to be applied to identify and reconstruct such events. A convenient solution relies on the acquisition of the complete waveform of the liquid scintillator signals. For this purpose, Flash ADC (FADC) with sampling rates as high as 1 GigaSample per second (GS/s), now becoming commercially available, can be used. They allow to record the waveform with the necessary accuracy, even for pulses of few nanoseconds width. The recorded waveforms can later be analyzed to extract particle type and energy, to obtain timing information, and to resolve overlapping signals. Some disadvantages, however, are still limiting the use of FADC in Nuclear Physics experiments: the large body of generated data, which often requires a large storage capability, the low resolution (8 bits) for the FADC with high sampling rate, the need of applying elaborated software procedures for signal reconstruction and, finally, the costs. Nevertheless, FADC may represent in some cases a more convenient, or even the only, solution for data acquisition, in particular, for measurements in high count-rate environment.

In this paper, we present the results of a FADC-based method for the acquisition and processing of signals produced in liquid scintillators detectors by γ-rays and neutrons. In Section 2, the shape of the signals for the two particle types is analyzed, resulting in a fitting procedure that allows to reproduce the signal waveform. In Section 3 the performance of the method in terms of energy reconstruction and n/γ discrimination is shown, while the pile-up identification and separation property of the method is discussed in Section 4. Conclusions are given in Section 5.

2. Pulse height analysis

The experimental setup consisted of a cylindrical cell of NE213 liquid scintillator 12.7 cm in diameter and 5.1 cm thick, coupled to a Philips XP2041 phototube, which was operated with an EG&G 2041 voltage divider. To reproduce the conditions typically encountered in measurements with particle beams, an RG58/U coaxial cable of 30 m length was used to transport the signal from the detector to the FADC. The Acqiris DP 110 [17] digitizer, with 1 GS/s sampling rate, 250 MHz bandwidth and 8 bit resolution, was used to record the waveform. The module was installed on a PCI bus of a 500 MHz PC equipped with Windows NT operating system. The data were subsequently transferred to a PC with Linux operating system, and analyzed with the PAW analysis package.

The pulse shape of a C_6D_6 scintillator, which will be used for measuring γ-rays from capture reactions at the CERN n_TOF facility, was investigated in a similar way. This detector consisted of a cylindrical cell with carbon fiber walls, 12 cm in diameter and 9 cm thick, read out by an EMI 9823QKA phototube (see Ref. [16] for more details).

Events were acquired from a ^{60}Co γ source and from an Am/Be neutron source, with an acquisition threshold on the FADC corresponding approximately to 200 keV electron-equivalent (the full scale was set to 2 MeV in the case of NE213 and 4 MeV for the C_6D_6). To extract the shape parameters for different particle types, signals from the ^{60}Co source were analyzed first, and their shape characterized. γ-rays from the Am/Be source were identified and separated from neutron-induced signals, which were subsequently analyzed.

2.1. Shape analysis of γ signals

Fig. 1 shows a typical signal produced in the NE213 by the ^{60}Co source, as recorded with the FADC, at 1 GS/s sampling rate (solid symbols). The start of the signal was defined, consistent with the operation of constant fraction discriminators (CFD), as the time when the signal reaches a fixed fraction of its maximum—in this case 20%—minus 2 ns. This definition seems appropriate not only in the fitting procedure described later, but also to extract timing information, needed for example, in neutron time-of-flight measurements.

As shown in Ref. [18], the signal shape from scintillation detectors can be obtained by convoluting the exponential decay spectrum of the scintillator with the response function of the PM tube and readout system. For the case of a single decay time, this results is the difference between two exponential terms, one of which relates to the equivalent RC time constant of the anode, connecting cable and input stage of the FADC, and the other to the decay constant of the scintillator light output (see Ref. [18] for details). In the case of liquid scintillators, however, a fit with only two exponential terms does not give satisfactory results, especially at times greater than 50 ns, as shown by the dashed curve in the figure. This is not unexpected, because of the characteristic slow decay component of liquid scintillators. It is therefore necessary to add a second exponential decay, convoluted with the response function of the system, to account for the longer tail in the signal. A more accurate reproduction of the pulse shape can be obtained with the functional form:

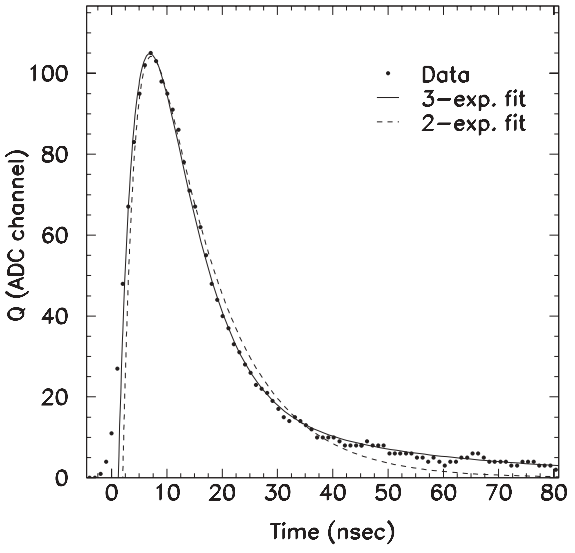

Fig. 1. Signal produced in the NE213 liquid scintillator cell by a γ-ray from the ^{60}Co source, acquired with a Flash ADC at 1 GHz sampling rate (solid symbols). The results of the fit performed with Eq. (2) of the text is shown by the solid line (the errors on each sample were assumed proportional to the square root of the ADC channel). The dashed line depict the results of a fit performed with only the first two exponential terms in Eq. (1).

$$L = A(e^{-\theta(t-t_0)} - e^{-\lambda_s(t-t_0)}) + B(e^{-\theta(t-t_0)} - e^{-\lambda_l(t-t_0)}). \quad (1)$$

The use of the additional free parameter t_0 for time reference is necessary, since the start of the signal, as defined above, is somewhat conventional and should be optimized for signal description.

A fit according to Eq. (1) with six free parameters (A, B, t_0, θ, λ_s and λ_l) is CPU time consuming and may not always easily converge to the best solution, the final convergence depending

on the initial parameters. To simplify and stabilize the fitting procedure, it would be desirable to reduce the number of free parameters by identifying their single best values or finding relations among them. For this purpose, the following procedure can be used:

(1) a significant number of events are fitted with Eq. (1), keeping all six parameters free;
(2) the distribution of the three exponential decay constants (θ, λ_s and λ_l) is determined, and an average value is extracted for these parameters;
(3) keeping the three exponential decay constants fixed, the events are fitted again searching only for the time reference t_0 and the normalization parameters A and B;
(4) an average value is chosen for t_0, and a relation between A and B is found, so that all events can be fitted with only one normalization constant.

The procedure was applied to 1000 γ-ray events of the ^{60}Co source detected with the NE213 liquid scintillator. The exponential decay constants θ, λ_s and λ_l, obtained from the six-parameter fit (first step), present a Gaussian-like distribution with a standard deviation of $\sim 10\%$. Once an average value is determined for these parameters, the events are fitted again with only the normalization constants A and B, and the time reference as free parameters. An average value is then chosen for t_0 and for the B/A ratio. As a result, only one free normalization parameter remains, and Eq. (1) for γ-rays can now be written as

$$L = A(e^{-(t-0.31)/5.578} - e^{-(t-0.31)/4.887} + 0.0166e^{-(t-0.31)/34.276}). \quad (2)$$

It should be noted that the convolution of the slow component with the response function of the system, that is the third term in Eq. (1), is much smaller than all other terms in this case, and can be neglected. Eq. (2) corresponds to signals of fixed shape but different pulse height, as one would expect for particles of the same type but different energies deposited in the detectors. The fits performed with Eq. (2) result in an average reduced, normalized χ^2 only 20% higher as compared to the value obtained with the six-parameter fits, thus demonstrating the correctness of the functional form and, in particular, of the exponentials chosen. This is also evident in Fig. 1, with the solid curve representing the results of the fit with Eq. (2). One can note that the exponential decay constants in Eq. (2) are slightly different from the values expected on the basis of the physical properties of the liquid scintillator, that is 3.7 and 32 ns for the reciprocal of λ_s and λ_l, respectively. An overall reasonable description of the pulse shape can be obtained by using these values for the two exponentials, convoluted with the response function of the system, but the fit fails to reproduce the leading edge and the tail of the signal. Most probably, the reason for this discrepancy is associated with the possible presence of distortions in the leading edge, and with the effect of a further fluorescence component characterized by a lifetime of 270 ns.

A similar approach to the one described above was used also in the analysis of the C_6D_6 detector. The values of the exponential decay times found for this scintillator are $1/\theta = 4.264$ ns, $1/\lambda_s = 3.886$ ns and $1/\lambda_l = 50.73$ ns. These values do not significantly differ from the known physical properties of the C_6D_6, and are comparable to the values of the NE213 detector. A larger difference is observed for the tail content, being the value of the normalization constant $B/A = 1.472 \times 10^{-3}$, nearly a factor of 10 lower.

2.2. Shape analysis of neutron signals

The procedure followed for γ's can be repeated for neutrons in order to find the best shape parameters for this type of signals. In principle, one may find different values for all five fixed parameters (the three decay constants, t_0 and the contribution of the slow component). We have verified, however, that the procedure applied to neutrons leads to essentially the same three exponentials as for γ-rays, while a significant change is observed only for the contribution of the third term. Since the decay constants of the scintillator do not depend on the particle type, the only expected difference between γ- and neutron-induced signals is due to the relative contributions of the fast and slow components. For the Am/Be

source, the first step of the procedure can, therefore, be skipped by assuming the same decay constants as for the ^{60}Co source. A three-parameter fit (the three being the time reference t_0 and the normalization constants A and B) reveals that two branches are observed in the A–B plane. Fig. 2 shows the B/A ratio as a function of A for events from the Am/Be source (the parameter A is related to the energy deposited in the detector by $E(\text{keV}) \sim 0.5$ A). This pattern is remarkably similar to the typical fast versus tail plot, obtained from double charge integration (see Ref. [10] for example), with the two branches corresponding to neutrons and γ's. The projection of the B/A ratio, lower panel of Fig. 2, shows two distinct peaks, the first one corresponding to the distribution obtained from the ^{60}Co source, and thus clearly related to the γ-rays emitted from the Am/Be source, as well as to environmental γ's and

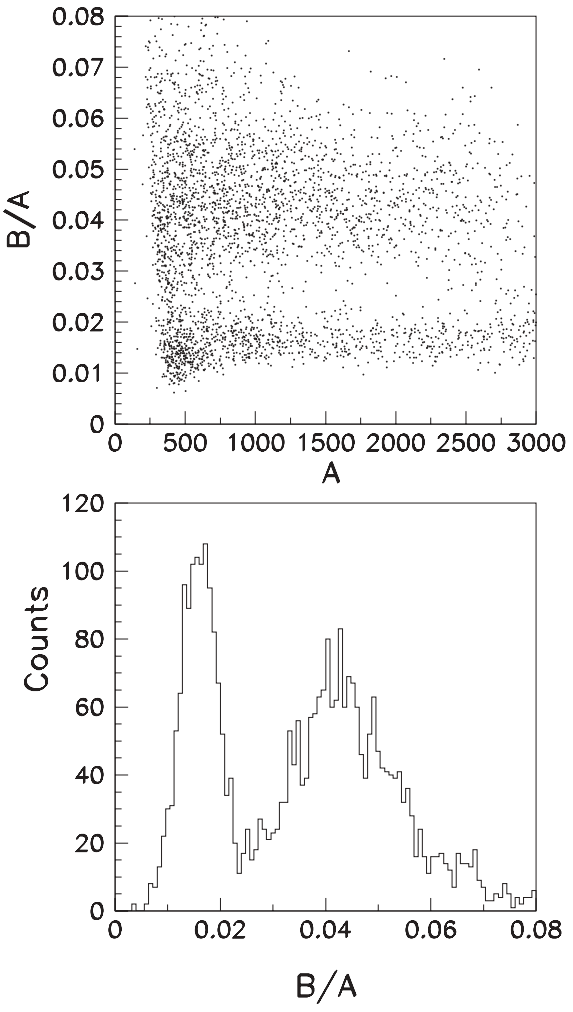

Fig. 2. Correlation between normalization constants for events from the Am/Be source detected in the NE213 scintillator. The upper and lower branch correspond to γ's and neutrons, respectively. The bottom panel shows the distribution of the B/A ratio. The first peak in the figure is similar to the peak of Fig. 3, and is therefore associated to γ's. The second peak corresponds to neutrons.

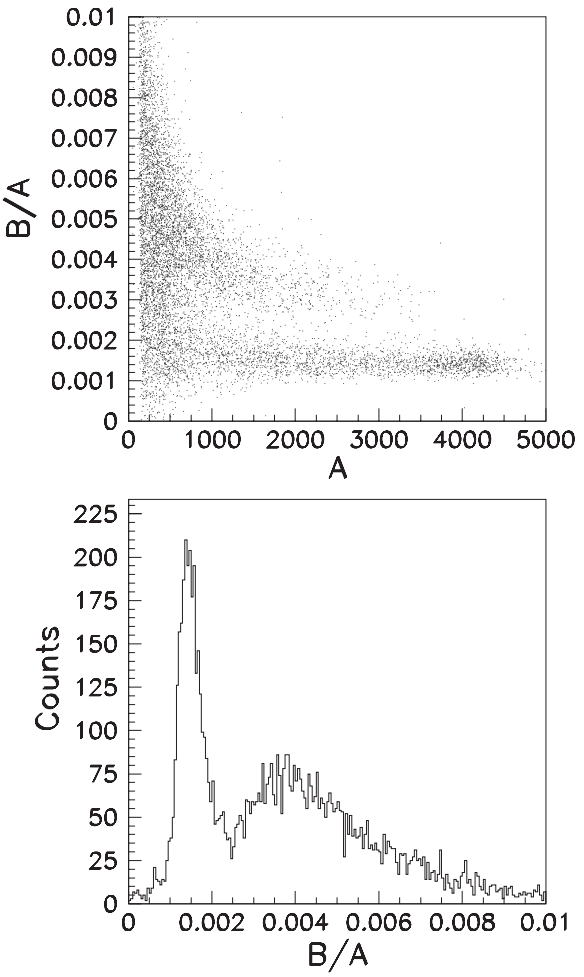

Fig. 3. Upper panel: the normalization constant of the slow component B/A versus the overall normalization constant, for events from the Am/Be in the C_6D_6-based liquid scintillator. The projection of the B/A ratio is shown in the bottom panel.

cosmic rays. The second peak corresponds to neutron events, due to the larger light content in the tail of signals from heavier particles. An average ratio of $B/A = 4.151 \times 10^{-2}$ is obtained for neutron events, compared to the value of 1.658×10^{-2} found for γ-rays.

The results of the shape analysis for the C_6D_6 detector are shown in Fig. 3 (the energy scale in this case is $E(\text{keV}) \sim 0.1$ A). In the upper panel the normalization constant of the slow component is plotted as a function of the signal amplitude for events from the Am/Be source, with the projection on the y-axis shown in the lower panel. As for NE213, the hardware threshold was kept around 200 keV, but a reasonable n/γ separation can be observed only above ~ 500 keV. As discussed later, because of the limited resolution of the FADC, the discrimination threshold is affected by the energy range used, which for the C_6D_6 was almost a factor of 2 higher than for the NE213.

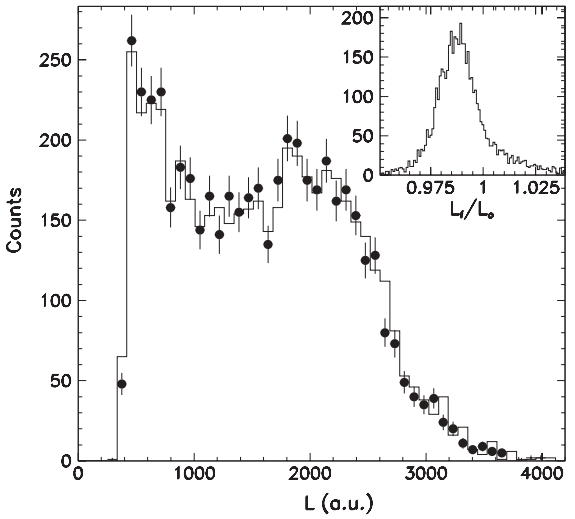

Fig. 4. Light output spectrum obtained from the ^{60}Co source with the NE213 detector. The symbols represent the results obtained by the analytical integral of the shape function given by Eq. (2), while the histogram is obtained by summing together all samples of the digitized signal. The inset shows the event-by-event ratio of the light outputs reconstructed with the two methods. The FWHM of the ratio is 2.2%.

3. Energy resolution and n/γ discrimination

As a quality check of the fit, we have compared the energy spectra obtained by the analytical integral of Eq. (2) up to 150 ns (L_f), to the result of numerical integration of the recorded light output in the same time range (L_o). Fig. 4 shows the energy spectra obtained for the ^{60}Co source. The solid symbols represent the result of the fitting procedure, while the histogram is obtained by summing together the samples of the digitized signal. The corresponding event-by-event ratio between the calculated light outputs is displayed in the inset. Both the spectra and the ratio indicate that the fit reproduces the signals reasonably well. In both cases, the observed resolution (extracted from analysing the Compton edge) is comparable to the one obtained with standard acquisition techniques by means of a charge sensing ADC.

The n/γ discrimination method is based on a comparison of the χ^2 values obtained with the parameters found for γ- and neutron-induced signals. For each event, two fits are performed with the shape functions of γ-rays and neutrons, respectively. The difference $D = \chi^2_\gamma - \chi^2_n$ of the corresponding normalized χ^2 values is expected to be negative in case of a γ-ray, and positive for a neutron. Fig. 5 shows the difference for events from the Am/Be source detected in the NE213 scintillator. For comparison, the shaded area represents the χ^2 difference for the ^{60}Co source. The discrimination capability is remarkably good all the way down to the hardware threshold of 200 keV. Although the actual limit of the identification method has not been investigated, the results here shown indicate that the discrimination power of the present method is comparable to other methods currently employed (zero cross-over time or double integration). A current limitation, however, is represented by the low resolution of the FADC (8 bits for commercially available fast modules), which hampers the accurate fit of the tail for signal amplitudes below 10% of the ADC range. This is illustrated by the analysis of the C_6D_6 detector (Fig. 3), which presents an identification threshold similar to the NE213 in ADC channels, but almost a factor of 2 higher in deposited energy, as expected from the larger energy range used with the C_6D_6.

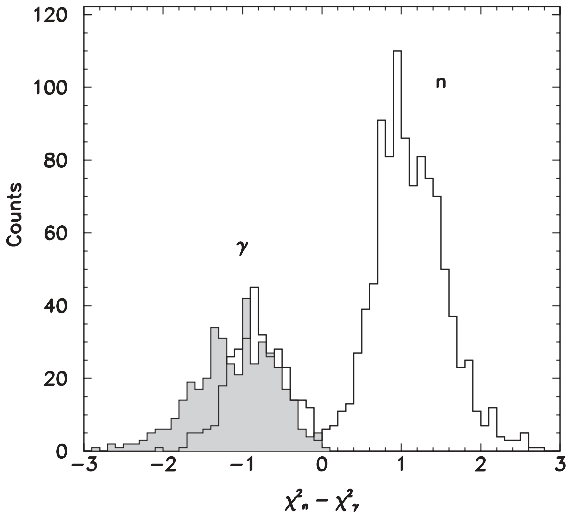

Fig. 5. Difference between the normalized χ^2's obtained by fitting the signals from the NE213 detector with the shape functions corresponding to γ's and neutrons (see text for details). The region of negative difference corresponds to γ-rays (or cosmic rays), while positive differences identify neutrons. The dashed area represents the n/γ discrimination pattern for a ^{60}Co source.

4. Treatment of pile-up events

The main advantage of using FADC for acquisition of signals from liquid scintillators resides in the possibility to identify and reconstruct pile-up events. Contrary to other hardware-based methods, the analysis of the entire pulse waveform in the presence of pile-up should, in principle, allow to disentangle the two overlapping signals and to provide reliable information on the type and energy of both particles giving rise to the pile-up event (provided that a minimum time separation exists between the two signals). The method proposed here consists in fitting the first signal up to the start of the second one. The analytical function obtained from the fit is subtracted, thus isolating the second (or later) signal, which can then be separately analyzed.

The reconstruction of both components in a pile-up event depends primarily on the time separation between the two signals, i.e. on the range in which the fit of the first signal can be performed. A minimum fit interval that still leads to stable results for the first signal was found to be around 40 ns. Nevertheless, one cannot say a priori what influence the subtraction of the first signal bears on the reconstruction of the second.

In order to check the accuracy of the method for pile-up identification and reconstruction, a large number of pile-up events was generated starting from individual signals recorded with the ^{60}Co source. Pairs of single events were randomly chosen and added together with a time separation varying between 20 and 100 ns in steps of 20 ns (the two individual signals were also stored in a separate file for comparison). First, a pile-up event is identified, and the time separation between the signals determined. The adopted criterion requires that two maxima are detectable within 250 ns after the start of the first signal (after this period the first signal has decayed to a negligible level, so that the occurrence of a second signal does not constitute a pile-up event). To avoid the misinterpretation of secondary maxima produced by fluctuations in the signal, mainly due to noise, positive and negative derivatives of at least 20% of the signal 4 ns before and after the maxima are required, respectively. After determining the position t_2 of the second maximum, a fit of the first signal is performed up to the start of the second signal (t_2—6 ns). The resulting analytical function is then subtracted from the original event, so that a fit of the remaining signal can be performed. Fig. 6 shows the result of this procedure for signals separated by 20 and 60 ns, respectively.

The accuracy of the pile-up identification and separation can be inferred, as before, by comparing the analytical integral of the fitting function L_f with the numerical integral of the two original signals L_o. In Fig. 7 the width of this ratio is plotted for both signals of the pile-up event as a function of the time difference between overlapping signals. Obviously, the uncertainty of the reconstruction is particularly large for small time differences, since the second signal is strongly affected by the tail of the first one. However, a separation of 40 ns seems to be sufficient to ensure the reliable analysis of both signals. Although a more detailed analysis should take into account, together with the time separation

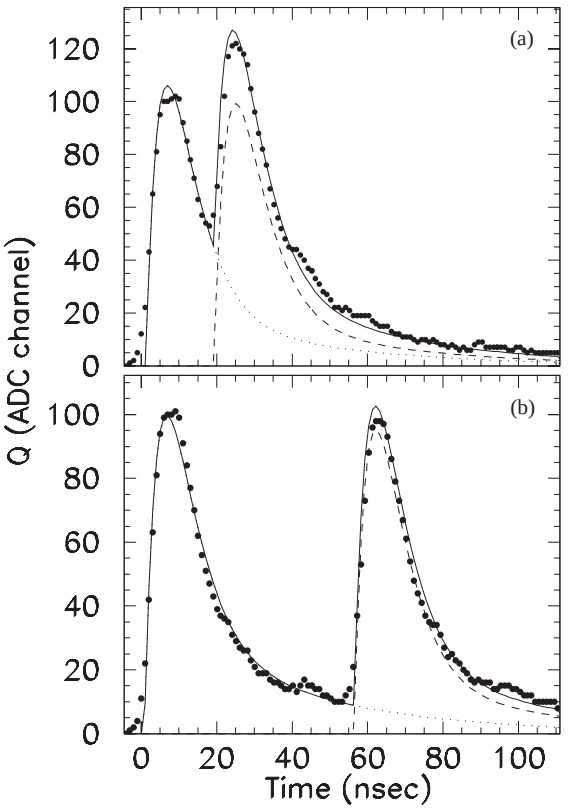

Fig. 6. Software-generated pile-up events for signal separations of 20 and 60 ns, respectively. The reconstructed pile-up pulse is shown in the figure (solid histogram), together with the individual fit functions (dotted and dashed histograms for the first and second pulse, respectively).

between signals, their relative amplitude, the results shown here provide some indications on the capability of the method to reconstruct pile-up events.

5. Conclusions

The possibility to acquire the signals of NE213 and C_6D_6 liquid scintillators by means of high-frequency FADC has been investigated. Once the pulse shape has been determined for γ's and neutrons, 1-parameter fits can be applied in order to extract information on the particle type and energy deposited. The accuracy of the method has

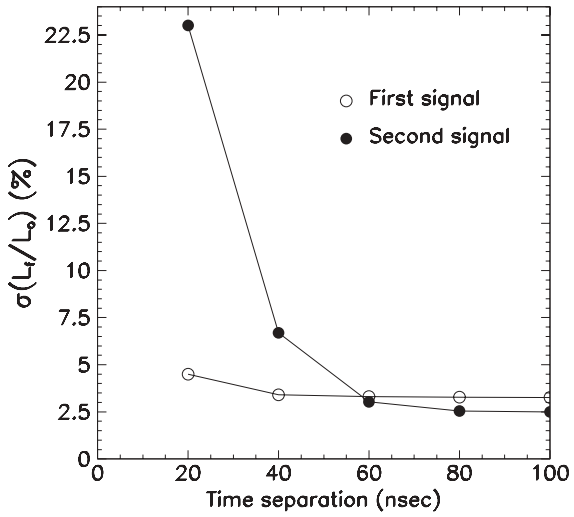

Fig. 7. For simulated pile-up events in the NE213 detector, the standard deviation of the ratio between the total charge of the reconstructed signals (L_f) and the charge of the original signals (L_o) is shown as a function of the time separation. L_f is obtained by analytical integration of the shape functions after fitting the pile-up signals, while L_o represents the numerical integral of each individual signal used to simulate the pile-up.

been validated by comparing the energy spectra and n/γ discrimination capability obtained from the fit with those obtained by numerical integration of the sampled signal. The performance of this innovative method, both in terms of energy resolution and particle identification is comparable to that of standard methods based on charge integration or zero crossing.

For software-generated pile-up events, the capability of the method to identify and reconstruct the individual signals has been tested. Contrary to typical electronic circuits for pile-up rejection, the recording of the original signal allows to disentangle and separate the overlapping signals in the pile-up event reliably, provided that their time difference exceeds 40 ns. The method presented here may be of advantage in studies with neutrons and γ-rays at high count rates, where an accurate identification and counting of all events is required. In view of these properties, signal reconstruction based on fast FADC will be used in high-resolution measurements of neutron cross-sections with C_6D_6 detectors at the new time-of-flight facility at CERN.

Acknowledgements

This work was supported by the EC under contract No. FIKW-CT-2000-00107.

References

[1] H. Laurent, et al., Nucl. Instr. and Meth. A 326 (1993) 517.
[2] N. Colonna, et al., Nucl. Instr. and Meth. A 381 (1996) 472.
[3] I. Tilquin, et al., Nucl. Instr. and Meth. A 365 (1995) 446.
[4] R.L. Macklin, J.H. Gibbons, Phys. Rev. 159 (1967) 1007.
[5] P. Sperr, et al., Nucl. Instr. and Meth. 116 (1974) 55.
[6] J. Kasagi, et al., Nucl. Instr. and Meth. A 236 (1985) 426.
[7] J.A. Adams, G. White, Nucl. Instr. and Meth. 156 (1978) 459.
[8] J.H. Heltsley, et al., Nucl. Instr. and Meth. A 263 (1988) 441.
[9] A. Bertin, et al., Nucl. Instr. and Meth. A 337 (1994) 445.
[10] D. Wolski, et al., Nucl. Instr. and Meth. A 360 (1995) 584.
[11] O. Barnaba, et al., Nucl. Instr. and Meth. A 410 (1998) 220.
[12] T. Okuda, et al., Nucl. Instr. and Meth. A 426 (1999) 497.
[13] K. Kamada, et al., Nucl. Instr. and Meth. A 426 (1999) 633.
[14] The nTOF collaboration, Proposal for a neutron time-of-flight facility, CERN/SPSC 99-08, SPSC/P310, March 1999.
[15] C. Rubbia, et al., CERN/AT/95-53 (ET) and CERN/AT/95-44 (ET).
[16] R. Plag, et al., in preparation.
[17] Acqiris Europe, 18 Chemin des Aulx, 1228 Plan-les-Ouates, Geneva, Switzerland.
[18] G. Knoll, Radiation Detection and Measurements, 3rd Edition, Wiley, New York, 2000.